International Journal of Bifurcation and Chaos, Vol. 27, No. 6 (2017) 1750091 (15 pages)

DOI: 10.1142/S0218127417500912

A Memristive Hyperchaotic Multiscroll Jerk System with Controllable Scroll Numbers

Chunhua Wang, Hu Xia* and Ling Zhou
College of Computer Science and Electronic Engineering,
Hunan University, Changsha 410082, P. R. China
*853200447@qq.com

Received November 24, 2016; Revised March 26, 2017

A memristor is the fourth circuit element, which has wide applications in chaos generation. In this paper, a four-dimensional hyperchaotic jerk system based on a memristor is proposed, where the scroll number of the memristive jerk system is controllable. The new system is constructed by introducing one extra flux-controlled memristor into three-dimensional multiscroll jerk system. We can get different scroll attractors by varying the strength of memristor in this system without changing the circuit structure. Such a method for controlling the scroll number without changing the circuit structure is very important in designing the modern circuits and systems. The new memristive jerk system can exhibit a hyperchaotic attractor, which has more complex dynamic behavior. Furthermore, coexisting attractors are observed in the system. Phase portraits, dissipativity, equilibria, Lyapunov exponents and bifurcation diagrams are analyzed. Finally, the circuit implementation is carried out to verify the new system.

Keywords: Hyperchaos; multiscroll attractor; memristor; circuit implementation.

1. Introduction

In recent years, the generation of chaotic attractors has become a hot topic in the investigation of chaos theory and application. Especially, multiscroll attractors have more complex dynamics than single-scroll and double-scroll chaotic attractors, and the generation of multiscroll chaotic system has been intensively researched (see e.g. [Suykens & Vandewalle, 1991; Tang *et al.*, 2011; Wang & Liu, 2008; Zhang, 2009; Sanchez-Lopez *et al.*, 2010; Wang *et al.*, 2013; Peng *et al.*, 2014]). The multiscroll chaotic system can be constructed by expanding the number of saddle focal equilibria with index 2. However, on the one hand, all the systems (see e.g. [Suykens & Vandewalle, 1991; Tang *et al.*, 2011; Wang & Liu, 2008; Zhang, 2009; Sanchez-Lopez *et al.*, 2010; Wang *et al.*, 2013; Peng *et al.*, 2014]) have only one positive Lyapunov exponent, and they belong to common chaotic systems. On the other hand, switch is used to control nonlinear function, which decides the number of saddle focal balance index of 2, so as to adjust the scroll number [Peng *et al.*, 2014]. The deficiency of this method is that gaining different scroll attractors will change the circuit structure. Moreover, switch is not conducive to integration.

Hyperchaos, which was first introduced by Rössler [1979], is defined as a chaotic attractor with at least two or more positive Lyapunov exponents. Compared with common chaos with only one positive Lyapunov exponent, hyperchaos can exhibit multidirectional expansion which leads to more complex and richer dynamical behaviors. Therefore, hyperchaotic systems have been intensively studied and are often considered better than common chaotic systems in the engineering fields, such as

*Author for correspondence

cryptosystem (see e.g. [Grassi & Mascolo, 1999; Wang & Zhang, 2016]), secure communication [Wu *et al.*, 2014], neural network (see e.g. [Zhang & Shen, 2014; Zhang *et al.*, 2015]), and laser design [Zunino *et al.*, 2011].

Hyperchaotic multiscroll attractors which have greater research value were recently proposed (see e.g. [Ahmad, 2006; Liu *et al.*, 2012]). Compared with common multiscroll chaotic system, hyperchaotic multiscroll attractor systems have more complex and richer dynamical behaviors. A hyperchaotic multiscroll attractor is constructed by adding multiple breakpoints to nonlinear section of the system [Ahmad, 2006]. However, the hyperchaotic multiscroll attractors proposed in the literature [Ahmad, 2006] were generated on the basis of an existing hyperchaotic system. This method is not suitable to obtain hyperchaotic multiscroll attractors based on common chaotic systems. By introducing time delay to the control function, a hyperchaotic attractor can be obtained in an existing multiscroll chaotic attractor from Chen system [Liu *et al.*, 2012]. Nevertheless, the feedback control function possesses four different parameters. The method creates trouble during the selection of parameters.

The concept of memristor as the fourth circuit element was first proposed by Leon Chua in 1971 [Chua, 1971]. It represents the relationship between charge and flux. Until 2008, researchers in Hewlett-Packard successfully fabricated a solid state implementation of memristor [Strukov *et al.*, 2008]. Since then, memristive chaotic systems have gained a lot of attention and success (see e.g. [Bao *et al.*, 2010a, 2010b, 2010c; Muthuswamy, 2010; Bao *et al.*, 2011; Iu *et al.*, 2011; Wang, 2012; Buscarino, 2012; Li & Zeng, 2013; Yu *et al.*, 2014; Chen *et al.*, 2015; Yang *et al.*, 2014]). Researchers mainly focused on using a quadratic or cubic nonlinear flux-controlled memristor to substitute Chua's diode of Chua's circuit (see e.g. [Bao *et al.*, 2010a, 2010b, 2010c; Muthuswamy, 2010; Bao *et al.*, 2011]), building types of memristor-based Chua's chaotic circuits and then completing the analysis of dynamics. Based on a nonlinear model of HP TiO_2 memristor, two different memristor-based chaotic circuits are constructed (see e.g. [Wang, 2012; Buscarino, 2012]). In addition, Li *et al.* proposed a memristor oscillator based on a twin-T network [Li & Zeng, 2013]. Through introducing a generalized memristor and a LC absorbing network into Wien-bridge oscillator, a kind of memristive Wien-bridge chaotic oscillator was proposed [Yu *et al.*, 2014]. A new charge-controlled memristor-based simplest chaotic circuit was deduced, and the circuit has only three basic elements [Chen *et al.*, 2015]. Recently, a new method of generating hyperchaotic attractor has been proposed. By replacing the resistor of Chua's circuit with a memristor, a four-dimensional hyperchaotic memristive system is obtained [Yang *et al.*, 2014]. However, it can only generate double-scroll attractor. A new memristor-based multiscroll hyperchaotic system is designed, various coexisting attractors and hidden coexisting attractors are observed in this system [Yuan *et al.*, 2016]. By utilizing a memristor to substitute a coupling resistor in the realization circuit of a three-dimensional chaotic system, a novel memristive hyperchaotic system with coexisting infinitely many hidden attractors is presented [Bao *et al.*, 2017]. A new type of flux-controlled memristor model with five-order flux polynomials is presented, and the memristor model is used to establish a memristor-based four-dimensional (4D) chaotic system, which can generate three-scroll chaotic attractor [Wang *et al.*, 2017].

In this paper, we propose a method to obtain hyperchaotic multiscroll attractor based on a memristor. By introducing a flux-controlled memristor to three-dimensional multiscroll jerk system, we can obtain a hyperchaotic memristive system with controllable number of scrolls. Compared with the methods (see e.g. [Ahmad, 2006; Liu *et al.*, 2012]), the method proposed in this paper is relatively easy to realize, and it can be easily extended to other three-dimensional chaotic systems. Compared with [Yang *et al.*, 2014], this present paper can achieve four-dimensional hyperchaotic multiscroll attractor, whereas [Yang *et al.*, 2014] realizes four-dimensional hyperchaotic double-scroll attractor. Compared with common multiscroll chaotic system with adjustable scroll [Peng *et al.*, 2014], the memristive jerk system just varies the strength of the memristor to get different scroll attractors, without changing the circuit structure. Moreover, by varying the strength of memristor, we can also find rich and complex dynamics, such as limit cycles, chaos, and even hyperchaos. Furthermore, coexisting attractors are observed in the memristive jerk system. The rest of this paper is organized as follows. In Sec. 2, the memristive jerk system and its phase portraits are described. In Sec. 3, the dynamical characteristics of memristive jerk system are analyzed. In Sec. 4, circuit implementation of the memristive jerk system with controllable number of scrolls is presented. In Sec. 5, some conclusions are finally drawn.

2. The Jerk System Based on a Memristor

The following jerk system proposed by J. C. Sprott (see e.g. [Sprott, 2000a, 2000b]) is considered

$$\begin{cases} \dot{x} = y \\ \dot{y} = z \\ \dot{z} = -y - \beta z + f(x) \end{cases} \tag{1}$$

where x, y and z are the state variables, β ($\beta = 0.45 \sim 0.7$) are system parameter and $f(x)$ is nonlinear function which decides the scroll number. When $f(x) = |x| - 1$, the jerk system generates single-scroll, as shown in Fig. 1(a). When $f(x) = \text{sgn}(x) - x$, the jerk system generates double-scroll, as shown in Fig. 1(b). Based on double-scroll jerk system, we can get multiscroll jerk system by expanding the number of saddle focal equilibria with index 2 in the x direction. Let $f(x) = F(x) - x$, according to the symmetry of nonlinear function, we can expand saddle focal balance with index 2 on both sides of the origin. The nonlinear function generating even-scroll is expressed as follows:

$$F_1(x) = A_1 \,\text{sgn}(x) + A_1 \sum_{n=1}^{N_1} \text{sgn}(x - 2nA_1) + A_1 \sum_{m=1}^{N_1} \text{sgn}(x + 2mA_1). \tag{2}$$

Nonlinear function generating odd-scroll is expressed as follows:

$$F_2(x) = A_2 \sum_{n=1}^{N_2} \text{sgn}(x - (2n-1)A_2) + A_2 \sum_{m=1}^{N_2} \text{sgn}(x + (2m-1)A_2). \tag{3}$$

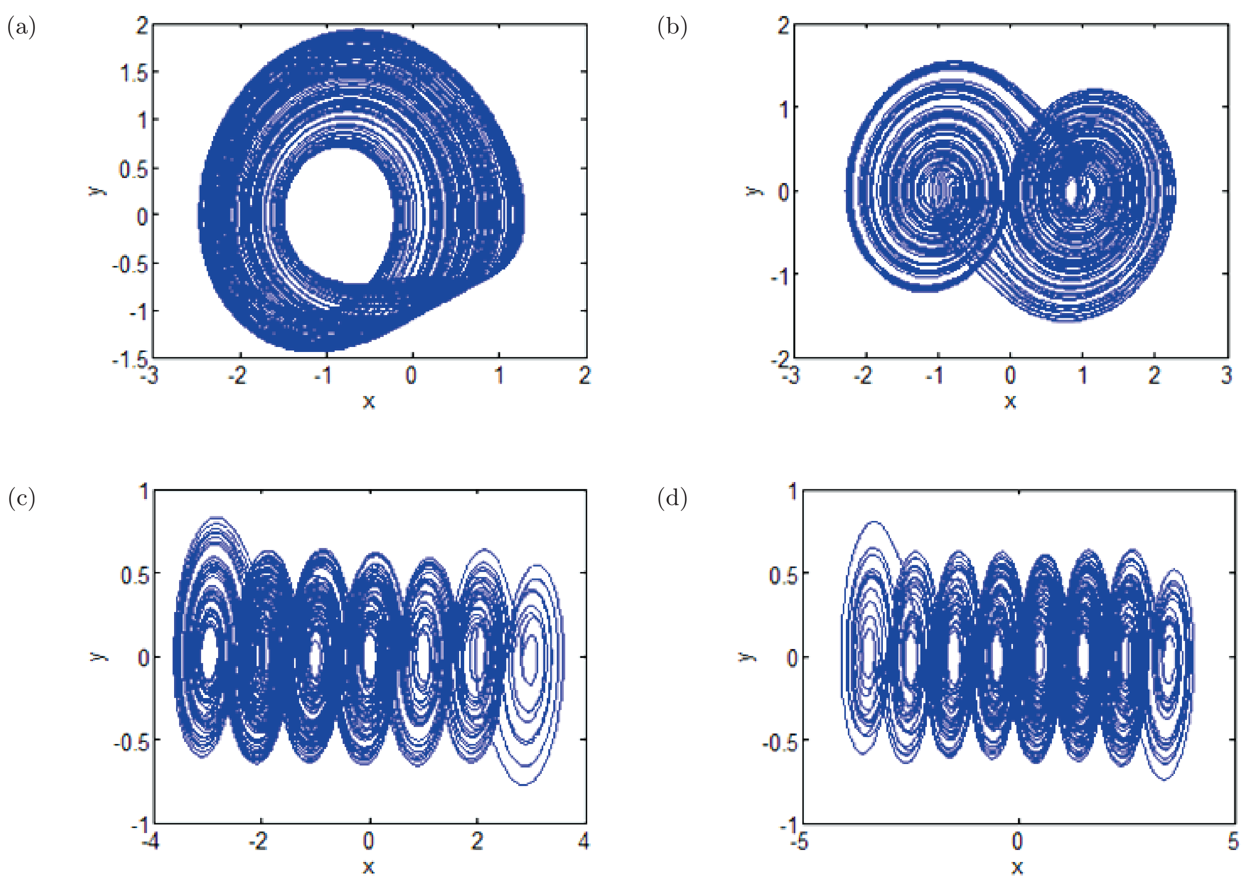

Fig. 1. The attractors of jerk system: (a) single-scroll, (b) double-scroll, (c) 7-scroll and (d) 8-scroll.

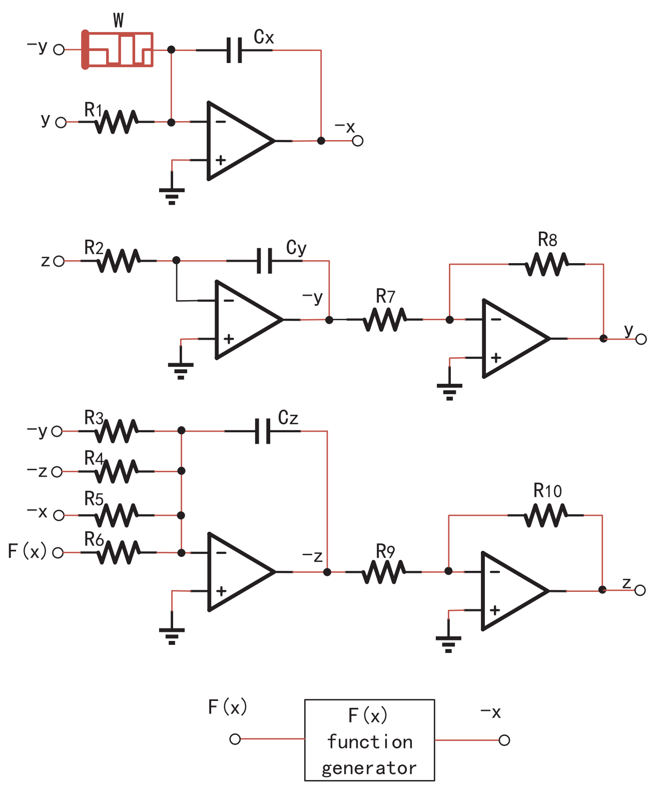

Fig. 2. Circuit implementation of the jerk system with a memristor.

Let $A_1 = A_2 = 0.5$ and $N_1 = N_2 = 3$, the system (1) can generate 7-scroll and 8-scroll chaotic attractors, as shown in Figs. 1(c) and 1(d).

If we use the variables x, y and z to denote voltages, then the state equations (4) can be easily achieved with an analog circuit, as shown in Fig. 2.

$$\begin{cases} C_x\dot{x} = \dfrac{y}{R_1} \\ C_y\dot{y} = \dfrac{z}{R_2} \\ C_z\dot{z} = -\dfrac{y}{R_3} - \dfrac{z}{R_4} - \dfrac{x}{R_5} + \dfrac{F(x)}{R_6}. \end{cases} \tag{4}$$

Let $\tau = t \cdot RC$ denote the physical time, where t is the dimensionless time, C is a reference capacitor, and R is a reference resistor, then the parameters of jerk system can be considered as follows: $C_x = C_y = C_z = C$, $R_1 = R_2 = R_3 = R_5 = R_6 = R$, $R/R_4 = \beta$.

To get a hyperchaotic memristive jerk system with controllable number of scrolls, we introduce a flux-controlled memristor, as illustrated by W in Fig. 2, to a three-dimensional multiscroll jerk system.

According to the definition of memristor [Chua, 1971], the memristor is a two-terminal nonlinear element with variable resistance. Its nonlinear relationship between the voltage across a flux-controlled memristor and the current into the memristor is given by $i = W(\varphi) \cdot v$, $\dot{\varphi} = v$, where $W(\varphi)$ is a memductance function. Therefore, we can gain the following state equation of the memristive jerk system:

$$\begin{cases} C_x\dot{x} = \dfrac{y}{R_1} - W(\varphi)y \\ C_y\dot{y} = \dfrac{z}{R_2} \\ C_z\dot{z} = -\dfrac{y}{R_3} - \dfrac{z}{R_4} - \dfrac{x}{R_5} + \dfrac{F(x)}{R_6} \\ \dot{\varphi} = y. \end{cases} \tag{5}$$

According to [Muthuswamy, 2010] and [Iu *et al.*, 2011], we use a quadric nonlinearity to indicate memductance function:

$$W(\varphi) = a + 3b\varphi^2 \tag{6}$$

where a and b are two positive constants. We obtain the following dimensionless equations:

$$\begin{cases} \dot{x} = y - \rho W(w)y \\ \dot{y} = z \\ \dot{z} = -y - \beta z - x + F(x) \\ \dot{w} = y \end{cases} \tag{7}$$

where ρ is a positive parameter indicating the strength of the memristor [Li *et al.*, 2015].

Let $\beta = 0.7$, $F(x) = F_1(x)$, we can get different even-scroll attractors when we increase ρ from 0 to 1, as shown in Table 1. Let $\beta = 0.7$, $F(x) = F_2(x)$, we can get different odd-scroll attractors when we increase ρ from 0 to 2, as shown in Table 1.

According to Table 1, the scroll number of the memristive jerk system proposed in this paper is controllable and is related to parameter ρ. When $F(x) = F_1(x)$, ρ changes from 0 to 1, the memristive jerk system can generate 8-scroll, 6-scroll, 4-scroll or double-scroll chaotic attractors. Different values of ρ correspond to different chaotic attractors respectively, which are shown in Fig. 3. When $F(x) = F_2(x)$, ρ changes from 0 to 2, the memristive jerk system can generate 7-scroll, 5-scroll, 3-scroll or single-scroll chaotic attractors. Different values of ρ, which are taken as 0.1, 0.21, 0.55, 2.0, correspond to

Table 1. The scroll number of memristive jerk system with different ρ.

Parameter	$F(x)$	ρ	The Scroll Number
$\beta = 0.7,\ A_{1,2} = 0.5,\ N_{1,2} = 3$	$F(x) = F_1(x)$	$\rho = 0.02$	8-scroll
		$\rho = 0.15$	6-scroll
		$\rho = 0.3$	4-scroll
		$\rho = 1.0$	Double-scroll
	$F(x) = F_2(x)$	$\rho = 0.1$	7-scroll
		$\rho = 0.21$	5-scroll
		$\rho = 0.55$	3-scroll
		$\rho = 2.0$	Single-scroll

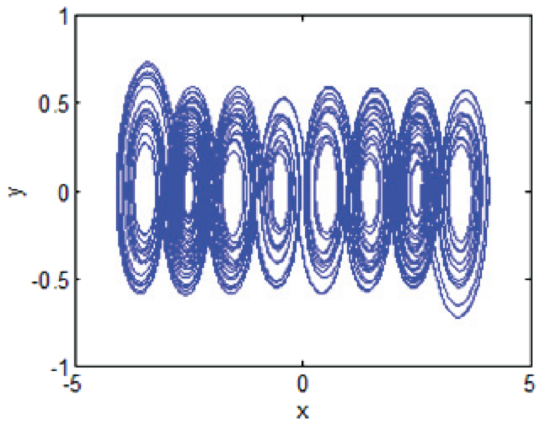

(a)

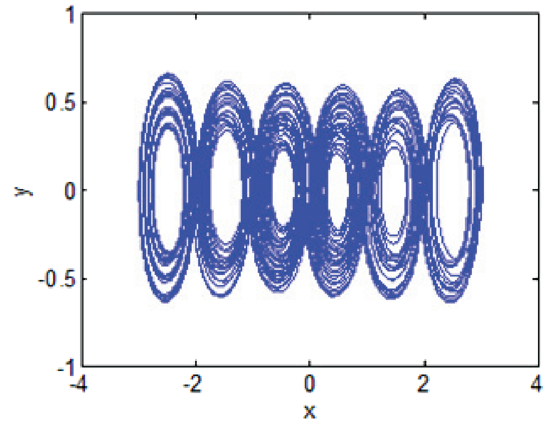

(b)

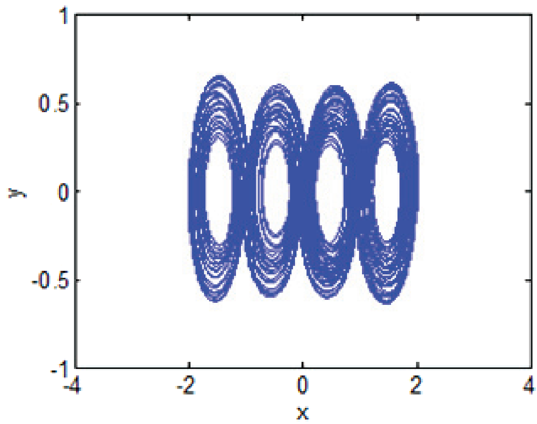

(c)

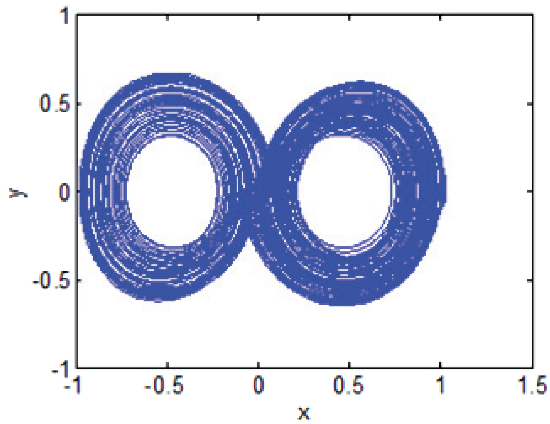

(d)

Fig. 3. Phase portraits of memristive jerk system with different ρ when $F(x) = F_1(x)$: (a) $\rho = 0.02$, (b) $\rho = 0.15$, (c) $\rho = 0.3$ and (d) $\rho = 1.0$.

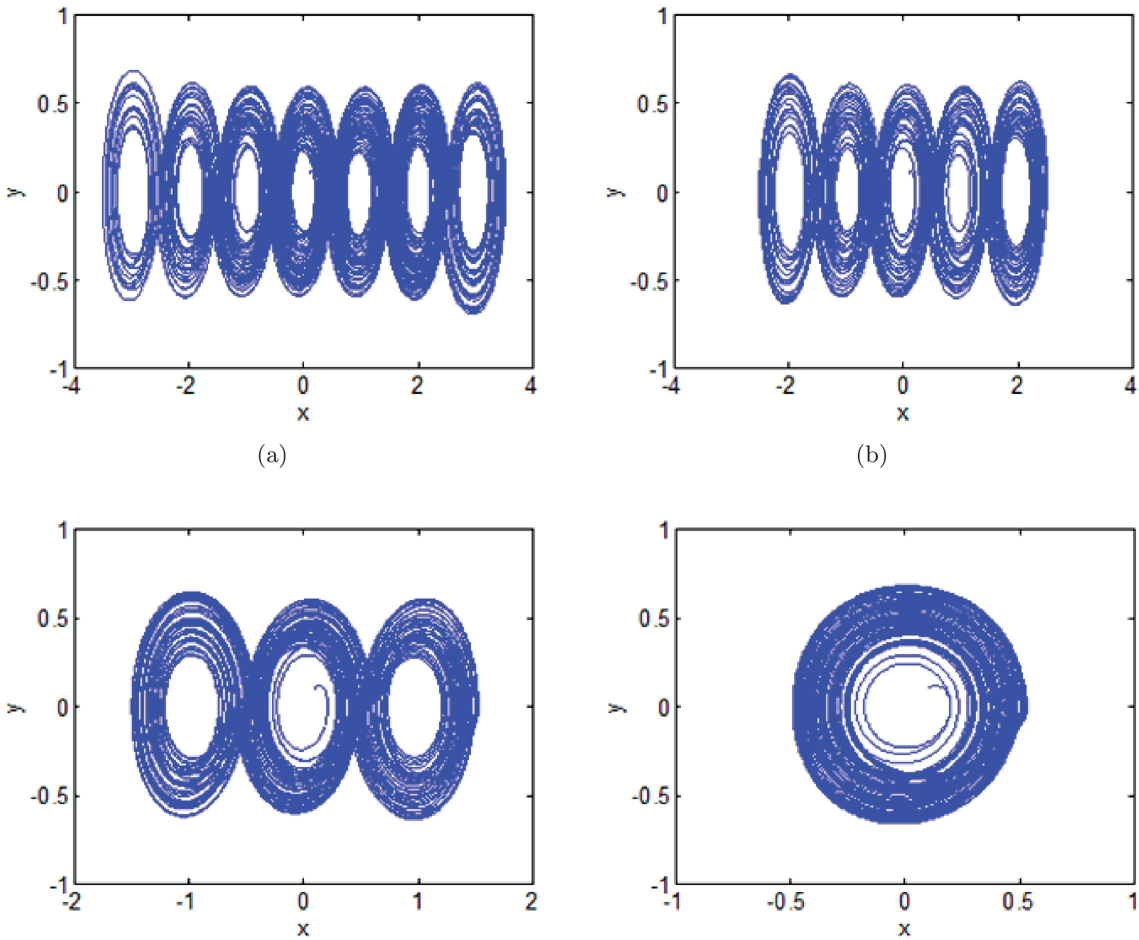

Fig. 4. Phase portraits of memristive jerk system with different ρ when $F(x) = F_2(x)$: (a) $\rho = 0.1$, (b) $\rho = 0.21$, (c) $\rho = 0.55$ and (d) $\rho = 2.0$.

different chaotic attractors respectively, which are shown in Fig. 4.

3. System Dynamics Analysis

3.1. *Dissipativity*

The dissipativity of system (7) can be described as

$$\nabla V = \frac{\partial \dot{x}}{\partial x} + \frac{\partial \dot{y}}{\partial y} + \frac{\partial \dot{z}}{\partial z} + \frac{\partial \dot{w}}{\partial w} = -\beta. \tag{8}$$

When $\beta > 0$, the memristive jerk system is obviously dissipative. This implies that asymptotic motion settles onto a chaotic attractor. Each volume containing the memristive jerk system trajectory shrinks to zero at an exponential rate as $t \to \infty$. Moreover,

$$\frac{dV}{dt} = e^{-\beta}. \tag{9}$$

It means that the volume of the chaotic attractor decreases by a factor of $e^{-\beta}$.

3.2. *Equilibrium point and stability analysis*

When introducing a memristor into the jerk system, the number and property of the equilibria will be greatly changed, which will be analyzed in detail as follows. Let $\dot{x} = \dot{y} = \dot{z} = \dot{w} = 0$, we can get

$$\begin{cases} y - \rho W(w)y = 0 \\ z = 0 \\ -y - \beta z - x + F(x) = 0 \\ y = 0. \end{cases} \tag{10}$$

When $F(x) = F_1(x)$, $N_1 = 3$, $A_1 = 0.5$, we can find that eight saddle focal equilibria with index 2 of jerk system change into the corresponding equilibria sets, $O_i = \{(x, y, z, w) \,|\, x = \pm(k - 0.5),\ y = z = 0, w = c\}$ $(k = 1, 2, 3, 4)$, where c can be any real constant value. We can obtain the Jacobian matrix on O_i

$$J_{O_i} = \begin{bmatrix} 0 & 1-\rho W(c) & 0 & 0 \\ 0 & 0 & 1 & 0 \\ -1 & -1 & -\beta & 0 \\ 0 & 1 & 0 & 0 \end{bmatrix}. \tag{11}$$

Its characteristic equation is given by

$$\lambda \cdot [\lambda^3 + \beta\lambda^2 + \lambda - \rho W(c) + 1] = 0 \tag{12}$$

where ρ and c are variable parameters, and the coefficient of cubic polynomial equation shown in the brackets of Eq. (12) are nonzero real constants. According to Routh–Hurwitz stable condition, when the relations of (13) are satisfied, all the roots of the cubic polynomial equation possess a negative real part. It means that the equilibria sets O_i are stable.

$$\begin{cases} -\rho W(c) + 1 > 0 \\ \beta - (-\rho W(c) + 1) > 0. \end{cases} \tag{13}$$

We can get the relationship between ρ and c,

$$\begin{cases} \sqrt{\dfrac{1-\beta-a\rho}{3b\rho}} < |c| < \sqrt{\dfrac{1-a\rho}{3b\rho}} \\ c_1 = \sqrt{\dfrac{1-\beta-a\rho}{3b\rho}} \\ c_2 = \sqrt{\dfrac{1-a\rho}{3b\rho}}. \end{cases} \tag{14}$$

According to Eqs. (14), if $c_1 < |c| < c_2$, the equilibria sets are stable. And if $|c| > c_2$ or $|c| < c_1$, the equilibria sets are unstable. Now if we take $a = 0.1$, $b = 0.05$, $\beta = 0.7$ and $\rho = 1.0$, then the two critical values from Eqs. (14) are

$$\begin{cases} c_1 = \sqrt{\dfrac{1-\beta-a\rho}{3b\rho}} = \dfrac{2\sqrt{3}}{3} \\ c_2 = \sqrt{\dfrac{1-\beta-a\rho}{3b\rho}} = \sqrt{6}. \end{cases} \tag{15}$$

We can choose a series of typical values of the constant c, the corresponding three nonzero characteristic roots λ_j $(j = 1, 2, 3)$ of the equilibria sets O_i are shown in Table 2.

Table 2. Different values of the constant c corresponding to the three nonzero characteristic roots.

$\|c\|$	λ_1	$\lambda_{2,3}$	Stability
0	-0.8196	$0.0598 \pm 1.0462i$	Unstable focus
$2\sqrt{3}/3$	-0.7	$0.0000 \pm 1.0000i$	Hopf bifurcation
2	-0.3419	$-0.1791 \pm 0.9195i$	Stable saddle
$\sqrt{6}$	0	$-0.3500 \pm 0.9367i$	Critical
3	0.3344	$-0.5172 \pm 1.0384i$	Unstable saddle
4	0.7322	$-0.7161 \pm 1.2393i$	Unstable saddle

When $F(x) = F_2(x)$, $N_2 = 3$, $A_2 = 0.5$, we can find that seven saddle focal equilibria with index 2 of jerk system change into the corresponding equilibria sets, $O_i = \{(x, y, z, w) \,|\, x = \pm k, y = z = 0, w = c\}$ $(k = 0, 1, 2, 3)$, where c can be any real constant value. The corresponding stability analysis of the equilibrium sets is consistent with the previous analysis.

3.3. *Lyapunov exponents and bifurcation diagrams*

In order to further explore the nonlinear dynamics of the memristive jerk system, we investigate the Lyapunov exponents and bifurcation diagrams. The Matlab simulation results are described in Figs. 5 and 6. By comparing Fig. 5 with Fig. 6, we can find that the Lyapunov exponents and the bifurcation diagrams match very well. Both of them can show that the memristive jerk system can generate complex dynamic behaviors.

When $F(x) = F_1(x)$, at the beginning, the memristive strength ρ is 0, and chaotic dynamics is initiated from the original jerk system, which is common chaotic behavior. The Lyapunov exponents are 0.13, 0.00, 0.00, and -0.85, respectively. With the strength ρ increasing from 0, the chaotic behavior is kept until $\rho \approx 0.57$. As the strength ρ increases from 0.57, more nonlinear behaviors have been found, such as limit cycles. A typical limit cycle can be observed at $\rho \approx 0.65$ and the Lyapunov exponents are 0, 0, -0.04, and -0.67, respectively. After the limit cycle behavior, chaos appears again at $\rho \approx 0.71$, and transits to hyperchaos at $\rho \approx 0.91$. A typical hyperchaos is at $\rho \approx 1.27$ and the Lyapunov exponents are 0.08, 0.03, 0, and -0.8, respectively. Clearly, the first two Lyapunov exponents are positive, so the attractor is hyperchaotic.

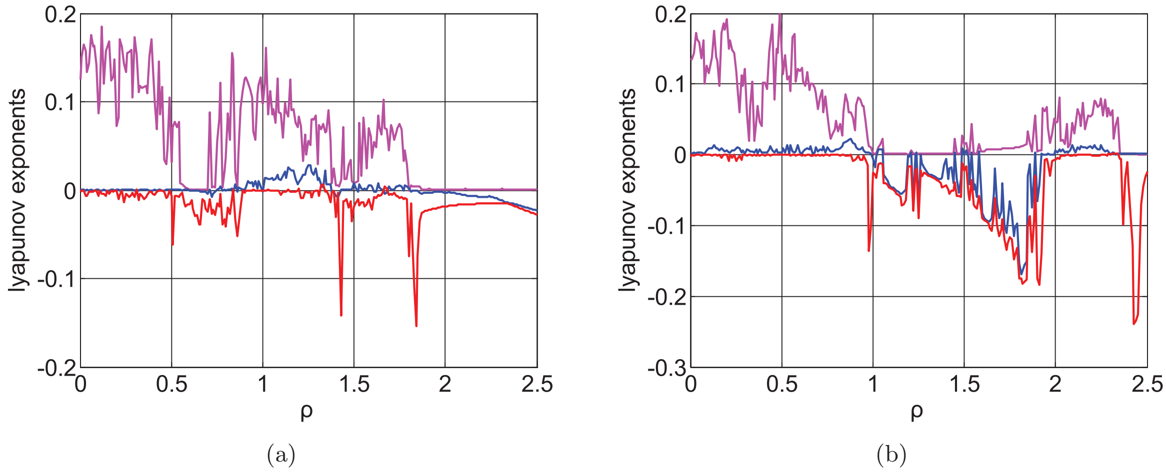

Fig. 5. First three Lyapunov exponents by adjusting ρ: (a) $F(x) = F_1(x)$ and (b) $F(x) = F_2(x)$.

When $F(x) = F_2(x)$, at the beginning, the memristive strength ρ is 0, and chaotic dynamics is also initiated from the original jerk system, which shows common chaotic behavior. The Lyapunov exponents are 0.12, 0.00, 0.00, and -0.82, respectively. With the strength ρ increasing from 0, chaos transits to hyperchaos at $\rho \approx 0.10$. A typical hyperchaos is at $\rho \approx 0.83$ and the Lyapunov exponents are 0.08, 0.02, 0, and -0.75, respectively. When the strength ρ keeps increasing from 1.06, periodic orbits begin to emerge until $\rho \approx 1.39$ except in some special interval. A typical periodic orbit can be observed at $\rho \approx 1.13$ and the Lyapunov exponents are 0, -0.04, -0.04, and -0.7, respectively. Further simulations show that the hyperchaotic attractor appears again at $\rho \approx 1.91$ and disappears at $\rho \approx 2.25$.

3.4. *Coexisting of multiple attractors relying on the memristor's initial condition*

Coexisting of multiple attractors imply two or more attractors in a system with the same parameter but different initial conditions. Coexistence of multiple attractors means that dynamical characteristics of nonlinear systems are sensitive to the changes of initial condition. Under initial conditions of the memristive jerk system (7) changing from $(0, 0.1, 0.1, 0.1)$ to $(0, 0.1, 0.1, 9.5)$ as Table 3, there appear new forms of chaotic attractors as shown in Figs. 7(a)–7(f). Coexistence of multiple attractors with a variable number of scrolls can be observed in the memristive jerk system (7). It is obvious from Fig. 7(a) that the memristive jerk system (7)

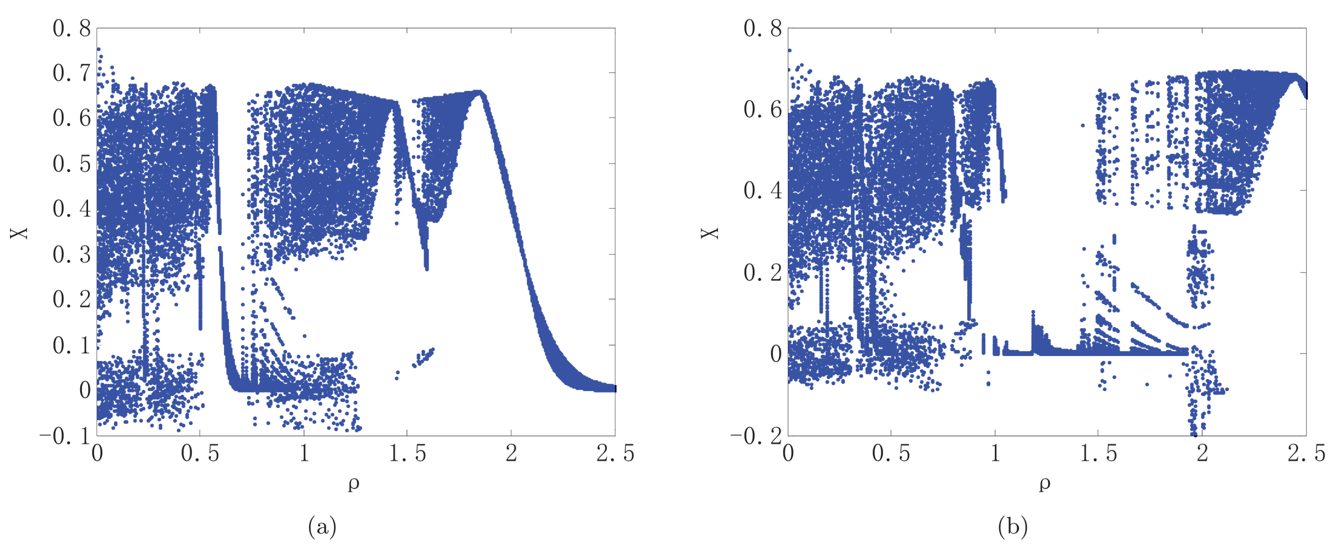

Fig. 6. Bifurcation diagram by adjusting ρ: (a) $F(x) = F_1(x)$ and (b) $F(x) = F_2(x)$.

Table 3. Coexisting attractors for various initial conditions of memristor.

Parameter	$F(x)$	ρ	Initial Conditions	Coexisting Attractors
$\beta = 0.7,\ A_{1,2} = 0.5,\ N_{1,2} = 3$	$F(x) = F_1(x)$	$\rho = 0.055$	$(0, 0.1, 0.1, 0.1)$	Fig. 7(a)
$\beta = 0.7,\ A_{1,2} = 0.5,\ N_{1,2} = 3$	$F(x) = F_1(x)$	$\rho = 0.055$	$(0, 0.1, 0.1, 2)$	Fig. 7(b)
$\beta = 0.7,\ A_{1,2} = 0.5,\ N_{1,2} = 3$	$F(x) = F_1(x)$	$\rho = 0.055$	$(0, 0.1, 0.1, 3)$	Fig. 7(c)
$\beta = 0.7,\ A_{1,2} = 0.5,\ N_{1,2} = 3$	$F(x) = F_1(x)$	$\rho = 0.055$	$(0, 0.1, 0.1, 4)$	Fig. 7(d)
$\beta = 0.7,\ A_{1,2} = 0.5,\ N_{1,2} = 3$	$F(x) = F_1(x)$	$\rho = 0.055$	$(0, 0.1, 0.1, 4.7)$	Fig. 7(e)
$\beta = 0.7,\ A_{1,2} = 0.5,\ N_{1,2} = 3$	$F(x) = F_1(x)$	$\rho = 0.055$	$(0, 0.1, 0.1, 9.5)$	Fig. 7(f)

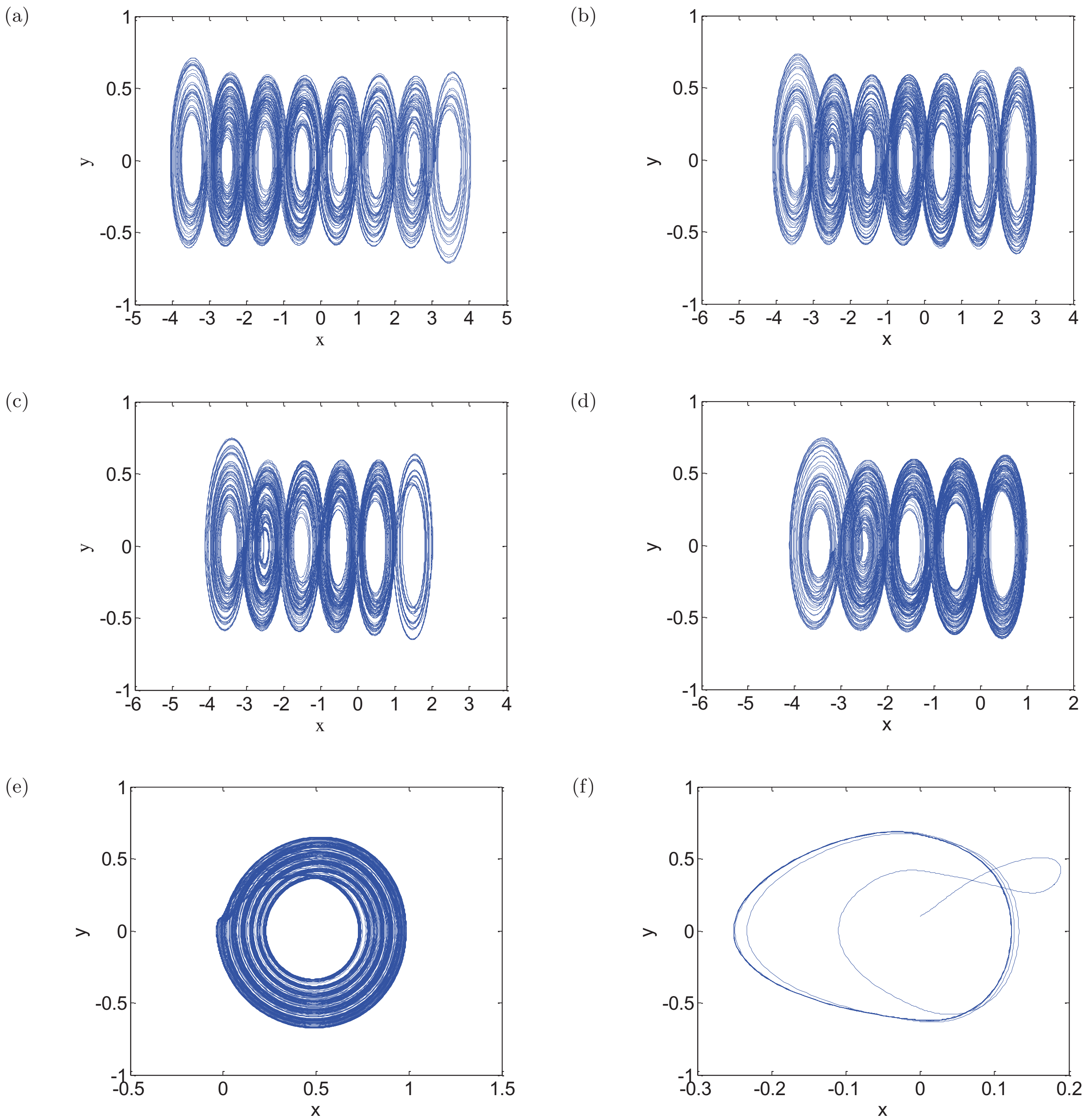

Fig. 7. Phase portraits of coexisting attractors in the x–y plane: (a) $(0, 0.1, 0.1, 0.1)$, (b) $(0, 0.1, 0.1, 2)$, (c) $(0, 0.1, 0.1, 3)$, (d) $(0, 0.1, 0.1, 4)$, (e) $(0, 0.1, 0.1, 4.7)$ and (f) $(0, 0.1, 0.1, 9.5)$.

has 8-scroll chaotic attractors within x varying in the interval $[-4, 4]$ for initial $(x, y, z, w) = (0, 0.1, 0.1, 0.1)$. It has 7-scroll chaotic attractors in Fig. 7(b) within x varying in the interval $[-4, 3]$ for initial $(x, y, z, w) = (0, 0.1, 0.1, 2)$. If the initial condition of the memristive jerk are set as $(x, y, z, w) = (0, 0.1, 0.1, 9.5)$, the x–y phase diagram is described in Fig. 7(f), and the memristor jerk system (7) enters the state of torus.

4. Circuit Implementation of the Memristive Jerk System

In order to further validate the memristive jerk system with controllable number of scrolls, we construct two analog circuits with classical components as shown in Figs. 8 and 9. In the circuit design, we use operational amplifier TL082CP and analog multiplier AD633JN, whose supply voltages are taken as $V_{EE} = \pm 15\,\text{V}$. The whole circuit shown in Fig. 8 consists of four modules. Each module is equivalent to realize a dimensionless equation in Eqs. (7). In the first module, two amplifiers U1, U2 and two multipliers G1, G2 are used to realize the memristive circuit. In the second module, the amplifier U3 is only used to implement the function of integration. In the third module, the usage of two amplifiers U4 and U5 is to realize the function of integration and inversion. In the last module, the amplifier U6 is used to realize the function of integration and addition. Its negative terminal is connected to a staircase wave circuit $F(x)$. The amplifier U7 is used to implement the function of inversion. The circuits of nonlinear function $F(x)$

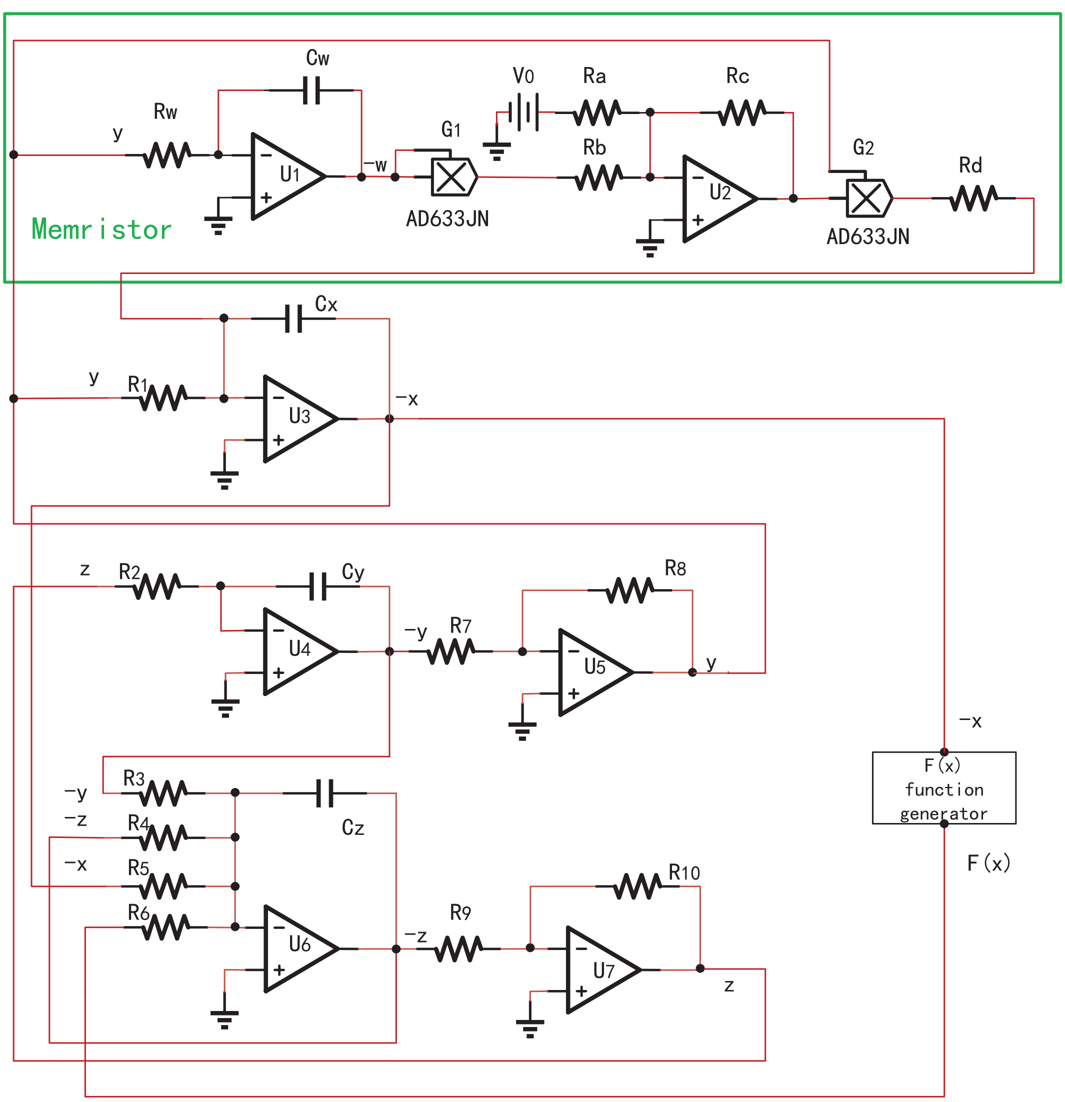

Fig. 8. The circuit of memristive jerk system.

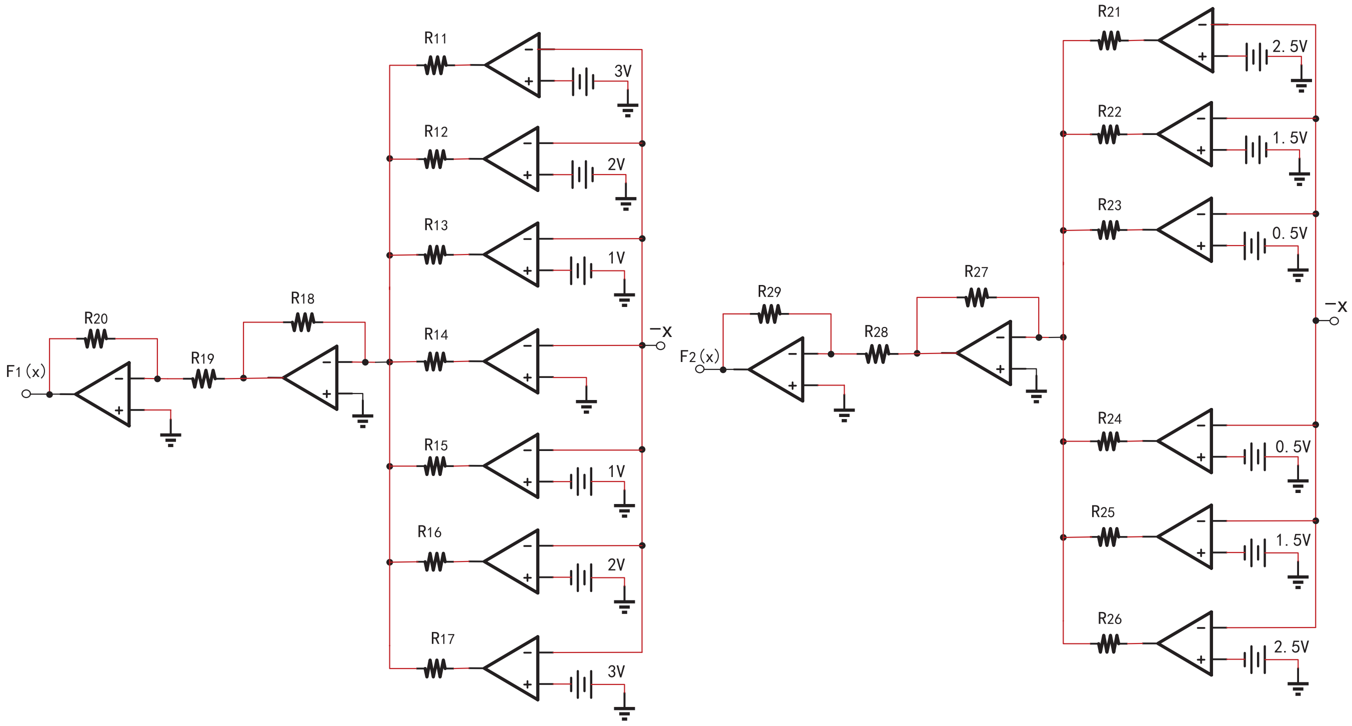

Fig. 9. The circuit of nonlinear function $F(x)$.

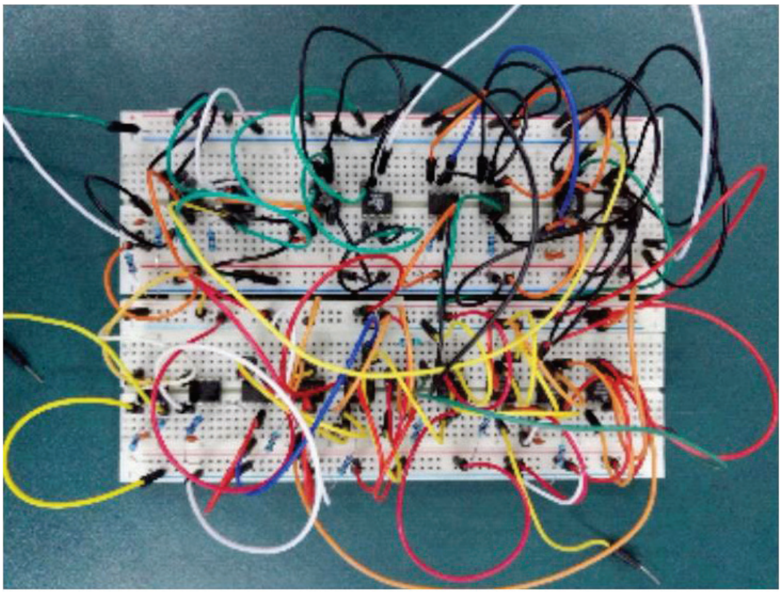

Fig. 10. The circuit experimental prototype of the memristive jerk system.

including $F_1(x)$ and $F_2(x)$ are described in Fig. 9. The experimental prototype is shown in Fig. 10.

Let $v_x = x$, $v_y = y$, $v_z = z$, $v_w = w$, where v_x, v_y, v_z and v_w are the voltages across capacitors. By setting a time scale factor RC on the dimensionless time and adding a multiplication factor 0.1/V on all multiplications with AD633JN, we can rewrite Eqs. (7) as follows:

$$\begin{cases} C\cdot\dot{v}_x = \dfrac{v_y}{R} - \left(\dfrac{0.1}{\mathrm{V}}\right)\cdot 10\rho \\ \qquad\qquad \cdot\left[\left(\dfrac{0.1}{\mathrm{V}}\right)\cdot 30b\cdot v_w\cdot v_w + a\right]\cdot\dfrac{v_y}{R} \\ C\cdot\dot{v}_y = \dfrac{v_z}{R} \\ C\cdot\dot{v}_z = -\dfrac{v_y}{R} - \dfrac{\beta v_z}{R} - \dfrac{v_x}{R} + \dfrac{F(v_x)}{R} \\ C\cdot\dot{v}_w = \dfrac{v_y}{R}. \end{cases} \tag{16}$$

By comparing Eqs. (16) with Eqs. (5), we can get the values of the capacitors and resistors of the circuit in Fig. 2 as follows:

$$\begin{cases} R_1 = R_2 = R_3 = R_5 = R_6 = R_7 \\ \quad = R_8 = R_9 = R_{10} = R \\ R_4 = \dfrac{R}{\beta} \\ C_x = C_y = C_z = C. \end{cases} \tag{17}$$

Let us take $R = 100\,\mathrm{k\Omega}$ and $C = 3.3\,\mathrm{nF}$. According to the parameters of the memristive jerk system, i.e. $\beta = 0.7$, we have $R_1 = R_2 = R_3 = R_5 = R_6 = 100\,\mathrm{k\Omega}$, $R_4 = 143\,\mathrm{k\Omega}$, $R_7 = R_8 = R_9 = R_{10} = 100\,\mathrm{k\Omega}$ and $C_x = C_y = C_z = 3.3\,\mathrm{nF}$. In the memristor, if we take $C_w = C$, $R_w = R$, $R_c = 100\,\mathrm{k\Omega}$ and $V_0 = 0.1\,\mathrm{V}$, then it is not hard to see that $R_d = R/10\rho$, $V_0R_c/R_a = a$, $R_c/R_b = 30b$. According to the above discussion, when $a = 0.1\,\mathrm{V}$ and $b = 0.05$, we can easily get the values of the two resistors: $R_a = 100\,\mathrm{k\Omega}$, $R_b = 66.7\,\mathrm{k\Omega}$.

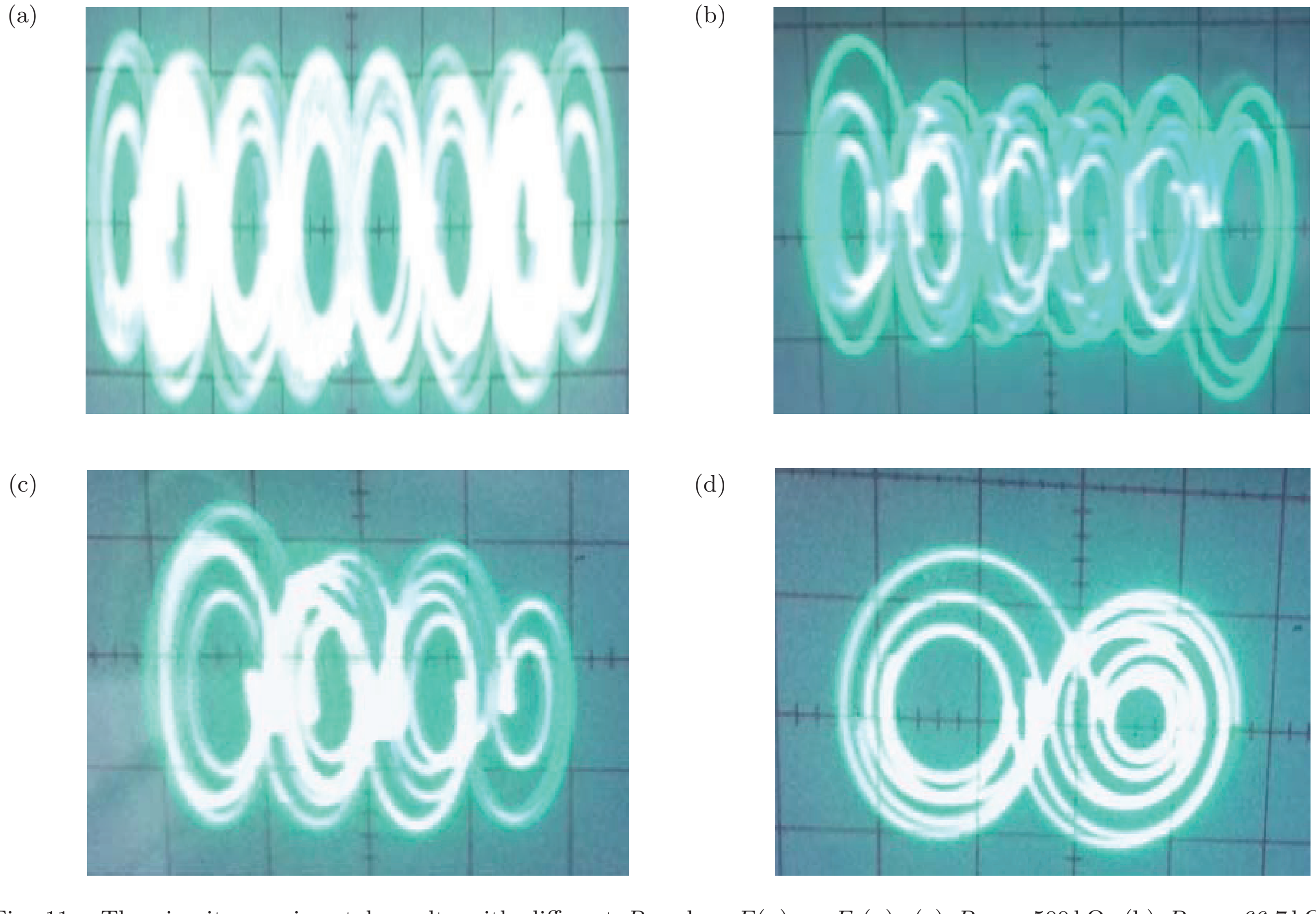

Fig. 11. The circuit experimental results with different R_d when $F(x) = F_1(x)$: (a) $R_d = 500\,\mathrm{k\Omega}$, (b) $R_d = 66.7\,\mathrm{k\Omega}$, (c) $R_d = 33.3\,\mathrm{k\Omega}$ and (d) $R_d = 10\,\mathrm{k\Omega}$.

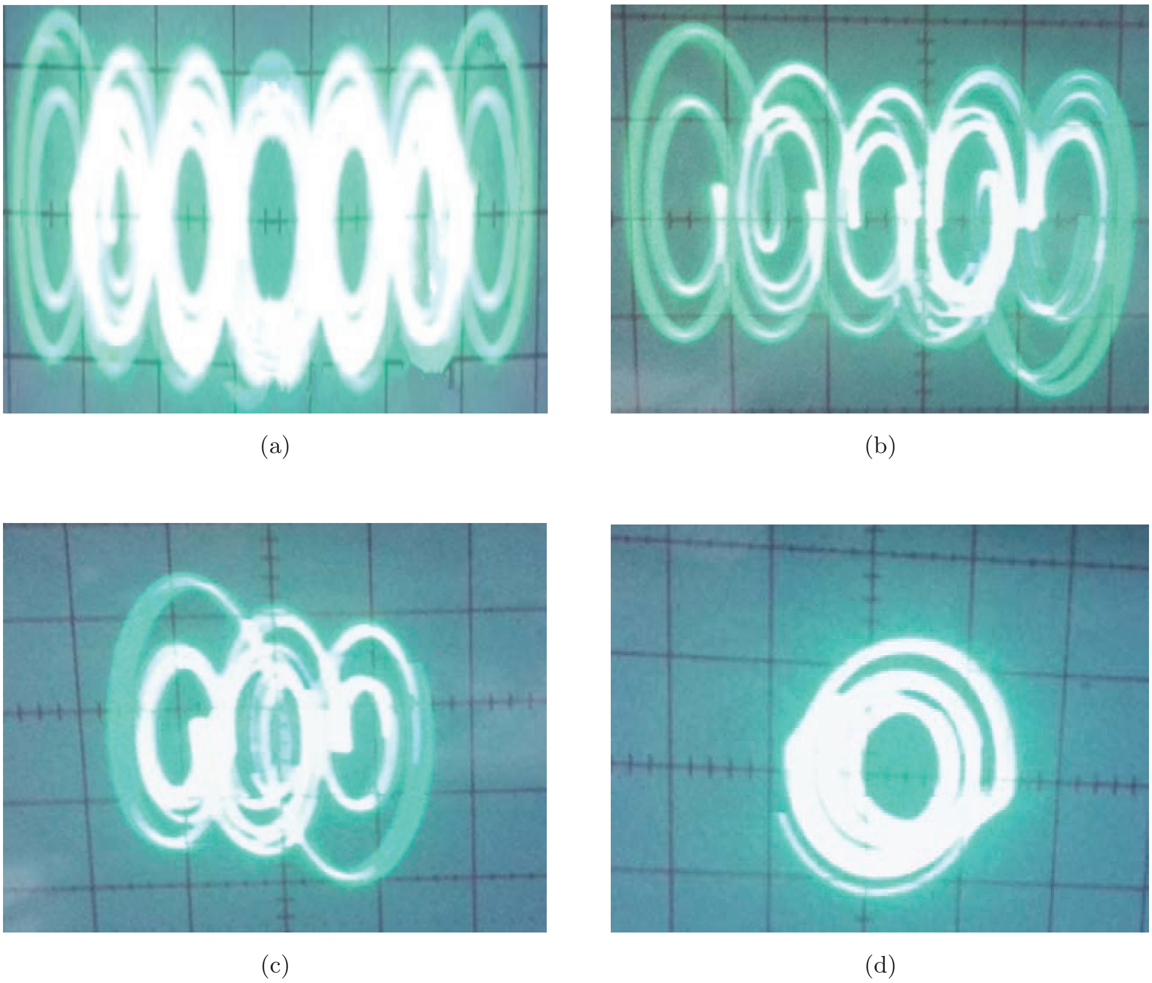

Fig. 12. The circuit experimental results with different R_d when $F(x) = F_2(x)$: (a) $R_d = 100\,\mathrm{k}\Omega$, (b) $R_d = 47.6\,\mathrm{k}\Omega$, (c) $R_d = 18.2\,\mathrm{k}\Omega$ and (d) $R_d = 5\,\mathrm{k}\Omega$.

Obviously, we can see that system parameter ρ is corresponding to circuit parameter R_d. By only changing the value of resistance R_d, we can easily control the scroll number of the memristive jerk system. The experimental results are shown in Figs. 11 and 12. We observe that the circuit experimental results of the memristive jerk system are consistent with the numerical simulation results.

5. Conclusions

In this paper, we have presented a new hyperchaotic memristive jerk system, which is modified from the jerk system. The main feature of this system is that we can get different scroll attractors by varying the strength of the memristor in this system, which is a significant difference from other chaotic systems reported before, where we must change the circuit structure to obtain different scroll attractors. Although the modification keeps the dissipativity of the original system, it brings the new system abundant complex dynamics, such as limit cycles, chaos, and even hyperchaos. Furthermore, coexisting attractors are observed in the memristive jerk system. The dynamics of the proposed chaotic system is investigated, including the stability of the equilibria, the numerical simulation of bifurcation and Lyapunov exponents. Theoretical analysis, numerical simulation and circuit experimental results have confirmed the effectiveness of this approach.

Acknowledgments

This work is supported by the National Natural Science Foundation of China (No. 61571185), the Natural Science Foundation of Hunan Province, China (No. 2016JJ2030) and the Open Fund Project of Key Laboratory in Hunan Universities (No. 15K027).

References

Ahmad, W. M. [2006] "A simple multi-scroll hyperchaotic system," *Chaos Solit. Fract.* **27**, 1213–1219.

Bao, B. C., Xu, J. P. & Liu, Z. [2010a] "Initial state dependent dynamical behaviors in a memristor based chaotic circuit," *Chinese Phys. Lett.* **27**, 51–53.

Bao, B. C., Liu, Z. & Xu, J. P. [2010b] "Dynamical analysis of memristor chaotic oscillator," *Acta Phys. Sin.* **59**, 3785–3793.

Bao, B. C., Liu, Z. & Xu, J. P. [2010c] "Transient chaos in smooth memristor oscillator," *Chinese Phys. B* **19**, 158–163.

Bao, B. C., Hu, W., Xu, J. P., Liu, Z. & Zou, L. [2011] "Analysis and implementation of memristor chaotic circuit," *Acta Phys. Sin.* **262**, 1775–1785.

Bao, B. C., Bao, H., Wang, N., Cen, M. & Xu, Q. [2017] "Hidden extreme multistability in memristive hyperchaotic system," *Chaos Solit. Fract.* **94**, 102–111.

Buscarino, A. [2012] "A chaotic circuit based on Hewlett–Packard memristor," *Chaos* **22**, 023136.

Chen, Z. Q., Tang, H., Wang, Z. L., Zhang, Q. & Han, J. W. [2015] "Design and circuit implementation for a novel charge-controlled chaotic memristor system," *J. Appl. Anal. Comput.* **5**, 251–261.

Chua, L. O. [1971] "Memristor: The missing circuit element," *IEEE Trans. Circuit Th.* **18**, 507–519.

Grassi, G. & Mascolo, S. [1999] "A system theory approach for designing cryptosystems based on hyperchaos," *IEEE Trans. Circuits Syst.-I: Fund. Th. Appl.* **46**, 1135–1138.

Iu, H. H. C., Yu, D. S., Fitch, A. L., Sreeram, V. & Chen, H. [2011] "Controlling chaos in a memristor based circuit using a Twin-T notch filter," *IEEE Trans. Circuits Syst.-I: Regul. Papers* **58**, 1337–1344.

Li, Z. J. & Zeng, Y. C. [2013] "A memristor oscillator based on twin-T network," *Chinese Phys. B* **22**, 148–153.

Li, Q. D., Zheng, H. Z. & Li, J. [2015] "Hyperchaos in a 4D memristive circuit with infinitely many stable equilibria," *Nonlin. Dyn.* **79**, 2295–2308.

Liu, X. Z., Shen, X. M. & Zhang, Z. T. [2012] "Multi-scroll chaotic and hyperchaotic attractors generated from Chen system," *Int. J. Bifurcation and Chaos* **22**, 215–224.

Muthuswamy, B. [2010] "Implementing memristor based chaotic circuits," *Int. J. Bifurcation and Chaos* **20**, 1335–1350.

Peng, Z. P., Wang, C. H. & Luo, X. W. [2014] "A novel multi-directional multi-scroll chaotic system and its CCII+circuit implementation," *Optik* **125**, 6665–6671.

Rössler, E. [1979] "An equation for hyperchaos," *Phys. Lett. A* **71**, 155–157.

Sanchez-Lopez, C. R., Trejo-Guerra, R., Munoz-Pacheco, J. M. & Tlelo-Cuautle, E. [2010] "N-scroll chaotic attractors from saturated function series employing CCII+s," *Nonlin. Dyn.* **61**, 331–341.

Sprott, J. C. [2000a] "Simple chaotic systems and circuits," *Amer. J. Phys.* **68**, 758–763.

Sprott, J. C. [2000b] "A new class of chaotic circuit," *Phys. Lett. A* **266**, 19–23.

Strukov, D. B., Snider, G. S., Stewart, D. R. & Williams, R. S. [2008] "The missing memristor found," *Nature* **453**, 80–83.

Suykens, J. A. K. & Vandewalle, J. [1991] "Generation of n-double scrolls ($n = 1; 2; 3; 4; \ldots$)," *IEEE Trans. Circuits Syst.-I* **40**, 861–867.

Tang, W. K. S., Zhong, G. Q. & Chen, G. [2011] "Generation of n-scroll attractors via sine function," *IEEE Trans. Circuits Syst.-I: Fund. Th. Appl.* **48**, 1369–1372.

Wang, F. Q. & Liu, C. X. [2008] "Generation of multi-scroll chaotic attractors via the saw-tooth function," *Int. J. Mod. Phys. B* **22**, 2399–2405.

Wang, L. D. [2012] "Memristor model and its application for chaos generation," *Int. J. Bifurcation and Chaos* **22**, 1250205-1–14.

Wang, C. H., Xu, H. & Yu, F. [2013] "A novel approach for constructing high-order Chua's circuit with multi-directional multi-scroll chaotic attractors," *Int. J. Bifurcation and Chaos* **23**, 1350022-1–10.

Wang, X. Y. & Zhang, H. L. [2016] "A novel image encryption algorithm based on genetic recombination and hyper-chaotic systems," *Nonlin. Dyn.* **83**, 333–346.

Wang, C. H., Xia, H. & Zhou, L. [2017] "Implementation of a new memristor-based multiscroll hyperchaotic system," *Pramana* **88**, 1–8.

Wu, X. J., Bai, C. X. & Kan, H. B. [2014] "A new color image cryptosystem via hyperchaos synchronization," *Commun. Nonlin. Sci. Numer. Simulat.* **19**, 1884–1897.

Yang, F. Y., Leng, J. L. & Li, Q. D. [2014] "The 4-dimensional hyperchaotic memristive circuit based on Chua's circuit," *Acta Phys. Sin.* **63**, 080502.

Yu, Q., Bao, B. C., Hu, F. W., Xu, Q. & Chen, M. [2014] "Wien-bridge chaotic oscillator based on first-order generalized memristor," *Acta Phys. Sin.* **63**, 240505.

Yuan, F., Wang, J. Y. & Wang, X. W. [2016] "Extreme multistability in a memristor-based multi-scroll hyper-chaotic system," *Chaos* **26**, 1–13.

Zhang, C. X. [2009] "Generation of grid multi-scroll Chua's chaotic attractors with combination of hysteresis and step series," *Acta Phys. Sin.* **58**, 120–130.

Zhang, G. D. & Shen, Y. [2014] "Exponential synchronization of delayed memristor-based chaotic neural networks via periodically intermittent control," *Neural Netw.* **55**, 1–10.

Zhang, G. D., Hu, J. H. & Shen, Y. [2015] "New results on synchronization control of delayed memristive neural networks," *Nonlin. Dyn.* **81**, 1167–1178.

Zunino, L., Rosso, O. A. & Soriano, M. C. [2011] "Characterizing the hyperchaotic dynamics of a semiconductor laser subject to optical feedback via permutation entropy," *IEEE J. Select. Top. Quant. Electron.* **17**, 1250–1257.